Journal of the Korean Nuclear Society
Volume 34, Number 5, pp.517~531, October, 2002

Speciation and Solubility of Major Actinides Under the Deep Groundwater Conditions of Korea

Dong-Kwon Keum, Min-Hoon Baik, and Pil-Soo Hahn
Korea Atomic Energy Research Institute
150 Dukjin-dong, Yuseong-gu, Daejeon 305-353, Korea
dkkeum@kaeri.re.kr

(Received June 20, 2002)

Abstract

The speciation and solubility of Am, Np, Pu and U have been analyzed by means of the geochemical code MUGREM, under the chemical conditions of domestic deep groundwater, in order to support the preliminary safety assessment for a Korean HLW disposal concept.

Under the conditions of groundwaters studied, the stable solid phase is $AmOHCO_3$(s) or $Am(OH)_3$(s), soddyite($(UO_2)_2SiO_2.2H_2O$) or $Na_2U_2O_7$(c), $Np(OH)_4$(am), and $Pu(OH)_4$(am) for Am, U, Np, and Pu, respectively. The dominating aqueous species are as follows: the complexes of Am(III), $Am(OH)_2^+$ and $Am(CO_3)_2^-$, the complexes of U(VI), $UO_2(OH)_3^-$ and $UO_2(CO_3)_3^{4-}$, the complexes of Np(IV), $Np(OH)_4$(aq) and $Np(OH)_3CO_3$, and the complexes of Pu(IV), $Pu(OH)_4$(aq) and $Pu(OH)_3CO_3^-$. The calculated solubilities exist between 1.9E-10 and 1.3E-9 mol/L for Am, between 5.6E-6 and 1.2E-4 mol/L for U, between 3.1E-9 and 1.3E-8 mol/L for Np, and between 6.6E-10 and 2.4E-10 mol/L for Pu, depending on groundwater conditions. The present solubilities of each actinide agree well with the results of other studies obtained under similar conditions.

Key Words : speciation, solubility, pH, Eh, carbonate, actinide, Am, Pu, Np, Pu

I. Introduction

The safe disposal of high-level radioactive waste (HLW) is a crucial step in the nuclear fuel cycle. One of the most widely accepted alternatives is the construction of underground facilities to accommodate the waste packages in a deep geologic formation (1). A safety assessment is to appraise radiological hazards arising from such a disposal. In the safety assessment the solubility of radionuclides is widely used as a source term to calculate radionuclides migration from repository. Likewise, the solubility limits under different chemical conditions might be used to design a repository that through its engineered barriers keeps the lowest possible radionuclide concentrations in the waters that eventually might intrude into it.

Actinides are specially interesting radionuclides in the safety assessment of HLW due to their radiological toxicity and long half-life period. The

solubility of actinides has been obtained from the experiments with solutions of relatively simple compositions compared with natural groundwater. It might be difficult to make direct estimation, based on these experimental measurements, of their solubilities in natural groundwater containing many kinds of complexing ions. The effects of coexisting aqueous species in solutions cannot be negligible to determine the solubility of a specific actinide. Therefore, the solubility and speciation of actinides in geochemical environments are subjected to calculations by using geochemical models, based on reliable thermodynamic data obtained from the experiments with solutions of relatively simple compositions. By this reason, there have been many attempts, using a geochemical code, to analyze the solubility and speciation of radionuclides including actinide, based on the measured characteristics of deep groundwater from candidate site (2~8). However, these studies exhibited different results for the most part due to the fact that the solubility of actinides significantly depends on the prevailing geochemical conditions of deep geological environments. This indicates that actinides solubility should be investigated, case-by-case, with a specific groundwater system, rather than generic approach.

In this study the aqueous solubility and speciation of Am, Np, Pu and U are analyzed, under the chemical conditions of domestic deep groundwater, in order to support the preliminary safety assessment for a Korean HLW disposal concept. Focused is especially the effect of pH, Eh and carbonate concentration, which are known to be the dominant factors controlling geochemical behaviors in granite groundwater system, on the solubility and speciation of actinides of interest.

2. Geochemical Model

2.1. Groundwaters

The chemical compositions of groundwaters

Table 1. Groundwater Compositions Used in the Study

GW / Species	Jungwon, Chungbuk J1(mol/L)	KAERI site, Yuseong, Daejeon[1)]		
		K1 (mol/L)	K1 (mol/L)	K3 (mol/L)
Na^+	1.35E-3	1.46E-3	1.50E-3	1.55E-3
K^+	1.28E-5	1.28E-5	2.30E-5	7.67E-6
Ca^{++}	1.85E-4	9.73E-5	8.73E-5	6.74E-5
Mg^{++}	8.23E-6	1.65E-6	1.65E-6	2.06E-6
SiO_2	3.23E-4	3.43E-4	4.42E-4	3.08E-4
Cl-	5.36E-5	1.21E-4	1.07E-4	1.18E-4
$[CO_3^{2-}]_T$	1.26E-3	3.23E-4	2.72E-4	4.09E-4
SO_4^{2-}	7.49E-5	2.08E-5	3.33E-5	2.40E-5
NO_3^-	4.84E-5	-	-	-
F-	3.47E-4	6.47E-4	6.53E-4	6.68E-4
TDS (mg/L)	168.0	96.7	101.2	101.3
pH	9.1	10.1	10.1	9.9
Eh (mV)	-136	-230	-155	-194
Depth (m)	400	321	416	458

1) In-situ and chemical data of the groundwater samples from the borehole YS-01 straddled by multipacker system in the Yuseong area (Sampling date: Jun. 2002)

measured from two local sites of Korea, Jungwon site (Chungbuk) and KAERI site (Yuseong, Daejeon), were used here as the reference. Table 1 shows the composition of groundwaters. The Jungwon groundwater was measured to depth of 400m. The groundwater is at pH 9.1 and has the redox potential (Eh) of -0.14V. The groundwaters sampled from KAERI site were obtained at three different depths of a single borehole by multipacker system. This is probably the first attempt using multipacker system to sample deep groundwater in Korea. The pH of KAERI site groundwater is about 10, and the redox potential have a relatively narrow band between -0.23 and -0.16 V. The total carbonate concentration is 1.26E-3 mol/L and 2.72E-4 to 4.09E-4 mol/L in Jungwon and KAERI site groundwater, respectively. The carbonate content of KAERI site groundwater seems to be a little lower than that of normal groundwater.

2.2. Geochemical Code and Thermodynamic Data

The speciation and solubility of actinides are usually calculated with a combination of geochemical equilibrium model and thermodynamic data obtained mostly by experiments. The present calculation has been performed by means of a geochemical code MUGREM, which was developed by KAERI. The code can deal with multi-geochemical equilibrium reaction system including aqueous complexation reactions, precipitation-dissolution reactions as well as adsorption reactions, and had been already verified through the comparison study of the calculation results with other code (9).

The geochemical code must be supported by thermodynamic data. There are tremendous thermodynamic data from different data sources (10~17). The comparison of data between different database shows rather large scatters in data for some species. The use of credible thermodynamic data is prerequisite for the reliable result. In Table 2 the aqueous complex formation constants of actinides used in this study are listed. Many parts of the reaction constants came from OECD/NEA thermodynamic data books (13,14,16). Furthermore, recent data of some species were incorporated through a peer review of expert by the joint study with FZK/INE, Germany (18). The present thermodynamic data can be characterized as follows; (A) the hydroxo-carbonate complexes of Np(IV) and Pu(IV) are incorporated. In the recent work by Neck and Kim (19), the ternary complexes of Np(IV) and Pu(IV) were observed by laser induced breakdown spectroscopy, and those species appeared to be predominant in neutral and alkaline regions. This is somewhat different from the other work (20), which withdraw those ternary species due to the lack of any experimental evidence, (B) the species $U(OH)_5$ was omitted as no experimental evidence has observed below pH 12, and (C) the polynuclear ternary complexes of U(VI), for example $(UO_2)_2CO_3OH$, were withdrawn because the existence of the species is ambiguous although these species are accepted in the NEA-TDB (13). These species usually came from potentiometric titration experiments under conditions exceeding the solubility. Under such oversaturation conditions it is questionable whether well-defined species will be formed. The ternary complexes observed in the experiment are suggested to be a kind of colloid of varying composition. At the present state those species cannot be identified correctly.

Solubility depends strongly on the state of the solid phase. Thermodynamically meaningful results require the information of a well-defined solid phase. Often actinide solids are initially precipitated in an amorphous state, and very

Table 2. Complex Formation Constant of Actinides Used in This Study

Actinides	Reaction	logβ	Ref.
Americium	$Am^{3+} + H_2O(l) - H^+ = AmOH_2^+$	-7.30	(26)
III	$Am^{3+} + 2H_2O(l) - 2H^+ = Am(OH)_2^+$	-15.19	(26)
	$Am^{3+} + 3H_2O(l) - 3H^+ = Am(OH)_3^\circ$	-25.69	(16)
	$Am^{3+} + F^- = AmF^{2+}$	3.40	(16)
	$Am^{3+} + 2F^- = AmF_2^+$	5.80	(16)
	$Am^{3+} + Cl^- = AmCl^{2+}$	0.24	(26)
	$Am^{3+} + 2Cl^- = AmCl_2^+$	-0.74	(26)
	$Am^{3+} + SO_4^{2-} = AmSO_4^+$	3.80	(16)
	$Am^{3+} + NO_3^- = AmNO_3^{2+}$	1.33	(16)
	$Am^{3+} + CO_3^{2-} = AmCO_3^+$	8.10	(26)
	$Am^{3+} + 2CO_3^{2-} = Am(CO_3)_2^-$	13.00	(26)
	$Am^{3+} + 3CO_3^{2-} = Am(CO_3)_3^{3-}$	15.20	(16)
	$Am^{3+} + 4CO_3^{2-} = Am(CO_3)_4^{5-}$	13.00	(26)
Uranium			
III	$U^{4+} + e^- = U^{3+}$	-9.35	(13)
IV	$U^{4+} + H_2O(l) - H^+ = UOH^{3+}$	-0.40	(22)
	$U^{4+} + 2H_2O(l) - 2H^+ = U(OH)_2^{2+}$	-1.09	(22)
	$U^{4+} + 3H_2O(l) - 3H^+ = U(OH)_3^+$	-4.69	(22)
	$U^{4+} + 4H_2O(l) - 4H^+ = U(OH)_4^\circ$	-9.99	(22)
	$6U^{4+} + 15H_2O(l) - 15H^+ = U_6(OH)_{15}^{9+}$	-16.90	(13)
	$U^{4+} + F^- = UF^{3+}$	9.28	(13)
	$U^{4+} + 2F^- = UF_2^{2+}$	16.20	(13)
	$U^{4+} + Cl^- = UCl^{3+}$	1.71	(13)
	$U^{4+} + SO_4^{2-} = USO_4^{2+}$	6.50	(13)
	$U^{4+} + NO_3^- = UNO_3^{3+}$	1.47	(13)
	$U^{4+} + CO_3^{2-} = UCO_3^{2+}$	13.70	(19)
	$U^{4+} + 2CO_3^{2-} = U(CO_3)_2^\circ$	24.30	(19)
	$U^{4+} + 3CO_3^{2-} = U(CO_3)_3^{2-}$	31.90	(19)
	$U^{4+} + 4CO_3^{2-} = U(CO_3)_4^{4-}$	35.10	(13)
	$U^{4+} + 5CO_3^{2-} = U(CO_3)_5^{6-}$	34.00	(13)
	$U^{4+} + 3H_2O(l) - 3H^+ + CO_3^{2-} = U(OH)_3CO_3^-$	-1.00	(13)
V	$U^{4+} + 2H_2O(l) - 4H^+ - e^- = UO_2^+$	-7.55	(13)
VI	$U^{4+} + 2H_2O(l) - 4H^+ - 2e^- = UO_2^{2+}$	-9.04	(13)
	$U^{4+} + 3H_2O(l) - 5H^+ - 2e^- = UO_2OH^+$	-14.74	(24)
	$U^{4+} + 4H_2O(l) - 6H^+ - 2e^- = UO_2(OH)_2(aq)$	-21.14	(24)
	$U^{4+} + 5H_2O(l) - 7H^+ - 2e^- = UO_2(OH)_3^-$	-29.04	(24)
	$U^{4+} + 6H_2O(l) - 8H^+ - 2e^- = UO_2(OH)_4^{2-}$	-41.44	(24)
	$2U^{4+} + 6H_2O(l) - 10H^+ - 4e^- = (UO_2)_2(OH)_2^{2+}$	-23.78	(24)
	$3U^{4+} + 11H_2O(l) - 17H^+ - 6e^- = (UO_2)_3(OH)_5^+$	-42.91	(24)
	$3U^{4+} + 13H_2O(l) - 19H^+ - 6e^- = (UO_2)_3(OH)_7^-$	-58.61	(24)
	$U^{4+} + 2H_2O(l) - 4H^+ - 2e^- + CO_3^{2-} = UO_2CO_3$	0.76	(23)
	$U^{4+} + 2H_2O(l) - 4H^+ - 2e^- + 2CO_3^{2-} = UO_2(CO_3)_2^{2-}$	7.66	(23)
	$U^{4+} + 2H_2O(l) - 4H^+ - 2e^- + 3CO_3^{2-} = UO_2(CO_3)_3^{4-}$	12.56	(23)

Actinides	Reaction	logβ	Ref.
Neptunium	$Np^{4+} + e^- = Np^{3+}$	3.70	(14)
III	$Np^{4+} + H_2O(l) - H^+ + e^- = NpOH^{2+}$	-3.1	(14)
	$Np^{4+} + 3CO_3^{2-} + e^- = Np(CO_3)_3^{3-}$	19.35	(14)
IV	$Np^{4+} + H_2O(l) - H^+ = NpOH^{3+}$	0.50	(22)
	$Np^{4+} + 2H_2O(l) - 2H^+ = Np(OH)_2^{2+}$	0.31	(22)
	$Np^{4+} + 3H_2O(l) - 3H^+ = Np(OH)_3^+$	-2.79	(22)
	$Np^{4+} + 4H_2O(l) - 4H^+ = Np(OH)_4^\circ$	-8.29	(22)
	$Np^{4+} + 3H_2O(l) - 3H^+ + CO_3^{2-} = Np(OH)_3CO_3^-$	6.03	(19)
	$Np^{4+} + 2H_2O(l) - 2H^+ + 2CO_3^{2-} = Np(OH)_2(CO_3)_2^{2-}$	16.96	(19)
	$Np^{4+} + 4H_2O(l) - 4H^+ + CO_3^{2-} = Np(OH)_4CO_3^-$	-4.57	(19)
	$Np^{4+} + 5CO_3^{2-} = Np(CO_3)_5^{6-}$	35.55	(14)
	$Np^{4+} + Cl^- = NpCl^{3+}$	1.50	(14)
	$Np^{4+} + SO_4^{2-} = NpSO_4^{2+}$	6.85	(14)
	$Np^{4+} + F^- = NpF^{3+}$	8.96	(14)
	$Np^{4+} + 2F^- = NpF_2^{2+}$	15.70	(14)
V	$Np^{4+} + 2H_2O(l) - 4H^+ - e^- = NpO_2^+$	-10.20	(14)
	$Np^{4+} + 3H_2O(l) - 5H^+ - e^- = NpO_2OH^\circ$	-21.5	(14)
	$Np^{4+} + 4H_2O(l) - 6H^+ - e^- = NpO_2(OH)_2^-$	-33.8	(14)
	$Np^{4+} + 2H_2O(l) - 4H^+ + SO_4^{2-} - e^- = NpO_2SO_4^-$	-9.76	(14)
	$Np^{4+} + 2H_2O(l) - 4H^+ + CO_3^{2-} - e^- = NpO_2CO_3^-$	-5.40	(25)
	$Np^{4+} + 2H_2O(l) - 4H^+ + 2CO_3^{2-} - e^- = NpO_2(CO_3)_2^{3-}$	-3.65	(25)
	$Np^{4+} + 2H_2O(l) - 4H^+ + 3CO_3^{2-} - e^- = NpO_2(CO_3)_3^{5-}$	-4.66	(25)
	$Np^{4+} + 3H_2O(l) - 5H^+ + 2CO_3^{2-} - e^- = NpO_2(CO_3)_2OH^{4-}$	-15.50	(14)
VI	$Np^{4+} + 2H_2O(l) - 4H^+ - 2e^- = NpO_2^{2+}$	-29.8	(14)
	$Np^{4+} + 3H_2O(l) - 5H^+ - 2e^- = NpO_2OH^+$	-34.9	(14)
	$2Np^{4+} + 6H_2O(l) - 10H^+ - 4e^- = (NpO_2)_2(OH)_2^{2+}$	-65.87	(14)
	$Np^{4+} + 2H_2O(l) - 4H^+ - 2e^- + CO_3^{2-} = NpO_2CO_3^\circ$	-20.48	(14)
	$Np^{4+} + 2H_2O(l) - 4H^+ - 2e^- + 2CO_3^{2-} = NpO_2(CO_3)_2^{2-}$	-13.28	(14)
	$3Np^{4+} + 6H_2O(l) - 12H^+ - 6e^- + 6CO_3^{2-} = (NpO_2)_3(CO_3)_6^{6-}$	-35.63	(14)
Plutonium	$Pu^{4+} + e^- = Pu^{3+}$	17.7	(14)
III	$Pu^{4+} + H_2O(l) - H^+ + e^- = PuOH^{++}$	10.8	(14)
	$Pu^{4+} + Cl^- + e^- = PuCl^{2+}$	18.90	(14)
IV	$Pu^{4+} + H_2O(l) - H^+ = PuOH^{3+}$	0.60	(22)
	$Pu^{4+} + 2H_2O(l) - 2H^+ = Pu(OH)_2^{2+}$	0.61	(22)
	$Pu^{4+} + 3H_2O(l) - 3H^+ = Pu(OH)_3^+$	-2.30	(22)
	$Pu^{4+} + 4H_2O(l) - 4H^+ = Pu(OH)_4^\circ$	-7.90	(22)
	$Pu^{4+} + SO_4^{2-} = PuSO_4^{2+}$	6.9	(14)
	$Pu^{4+} + CO_3^{2-} = PuCO_3^{2+}$	13.60	(19)
	$Pu^{4+} + 2CO_3^{2-} = Pu(CO_3)_2^\circ$	24.00	(19)
	$Pu^{4+} + 3CO_3^{2-} = Pu(CO_3)_3^{2-}$	31.50	(19)
	$Pu^{4+} + 4CO_3^{2-} = Pu(CO_3)_4^{4-}$	34.50	(19)

Actinides	Reaction	logβ	Ref.
	$Pu^{4+} + 5CO_3^{2-} = Pu(CO_3)_5^{6-}$	32.80	(19)
	$Pu^{4+} + 2H_2O(l) - 2H^+ + 2CO_3^{2-} = Pu(OH)_2(CO_3)_2^{2-}$	18.40	(19)
	$Pu^{4+} + 3H_2O(l) - 3H^+ + CO_3^{2-} = Pu(OH)_3CO_3^-$	6.00	(19)
	$Pu^{4+} + 4H_2O(l) - 4H^+ + CO_3^{2-} = Pu(OH)_4CO_3^{2-}$	-4.90	(19)
	$Pu^{4+} + 4H_2O(l) - 4H^+ + 2CO_3^{2-} = Pu(OH)_4(CO_3)_2^{4-}$	-3.50	(19)
	$Pu^{4+} + Cl^- = PuCl^{3+}$	1.80	(14)
	$Pu^{4+} + F^- = PuF^{3+}$	8.84	(14)
V	$Pu^{4+} + 2H_2O(l) - 4H^+ - e^- = PuO_2^+$	-17.5	(14)
	$Pu^{4+} + 2H_2O(l) - 4H^+ + CO_3^{2-} - e^- = PuO_2CO_3^-$	-12.38	(14)
	$Pu^{4+} + 2H_2O(l) - 4H^+ - e^- + 3CO_3^{2-} = PuO_2(CO_3)_3^{5-}$	-12.48	(14)
VI	$Pu^{4+} + 2H_2O(l) - 4H^+ - 2e^- = PuO_2^{2+}$	-33.3	(14)
	$Pu^{4+} + 3H_2O(l) - 5H^+ - 2e^- = PuO_2OH^+$	-38.8	(14)
	$Pu^{4+} + 4H_2O(l) - 6H^+ - 2e^- = PuO_2(OH)_2^o$	-46.5	(14)
	$2Pu^{4+} + 6H_2O(l) - 10H^+ - 4e^- = (PuO_2)_2(OH)_2^{2+}$	-74.1	(14)
	$Pu^{4+} + 2H_2O(l) - 4H^+ - 2e^- + SO_4^{2-} = PuO_2SO_4$	-29.9	(14)
	$Pu^{4+} + 2H_2O(l) - 4H^+ - 2e^- + CO_3^{2-} = PuO_2CO_3$	-23.9	(23)
	$Pu^{4+} + 2H_2O(l) - 4H^+ - 2e^- + 2CO_3^{2-} = PuO_2(CO_3)_2^{2-}$	-18.4	(23)
	$Pu^{4+} + 2H_2O(l) - 4H^+ - 2e^- + 3CO_3^{2-} = PuO_2(CO_3)_3^{4-}$	-15.8	(23)
	$Pu^{4+} + 2H_2O(l) - 4H^+ - 2e^- + Cl^- = PuO_2Cl^+$	-32.6	(14)
	$Pu^{4+} + 2H_2O(l) - 4H^+ - 2e^- + F^- = PuO_2F^+$	-28.74	(14)

slowly transform into the thermodynamically stable crystalline state. It is known that the stable solids in natural granite groundwater exist mainly as hydroxide, oxide, and carbonate owing to the low concentration of other salts such as nitrate, sulfate and phosphate. The actinides solids and their solubility product used in this study are listed in Table 3. The solubility limiting solid phase of each actinide under the present groundwater conditions was selected based on the solid stability diagram constructed with the solubility product constants.

3. Results and Discusion

Figures 1 to 7 show the aqueous speciation and stable solid phase of Am, U, Np, and Pu as functions of key parameters of granitic groundwater system. Table 4 lists the calculated solubility of each actinide under the present groundwater compositions. In all calculations, the closed-system system with respect to atmosphere was assumed to represent a deep geological environment.

3.1. Americium

In natural groundwater, the aqueous species as well as solids phase of americium exists only as the trivalent state, and therefore, the redox potential is not a function of the speciation and solubility of Am. Figure 1 shows (a) the HCO_3^- - pH diagram for aqueous speciation and (b) the solid stability field of americium, respectively. The Am-carbonates are predominant in higher carbonate concentration, whereas its hydroxo-complexes are in lower carbonate concentration. J1 groundwater falls into the region where $Am(CO_3)_2^-$ is the dominating aqueous species, whereas KAERI site groundwater exists near the boundary of the

Table 3. Solids and Their Solubility Product of Actinides Used in This Study

Actinides	Reaction	pK_{sp}	Ref.
Am	$Am^{3+} + 3H_2O - 3H^+ = Am(OH)_3$ (s)	-15.2	(16)
	$2Am^{3+} + 3CO_3^{2-} = Am_2(CO_3)_3$	33.4	(16)
	$Am^{3+} + H_2O - 2H^+ + HCO_3^- = AmOHCO_3$ (c)	-1.6	(26)
	$Am^{3+} + Na^+ - 2H^+ + 2HCO_3^- = AmNa(CO_3)_2$	-0.3	(26)
Np	$Np^{4+} + 4H_2O(l) - 4H^+ = Np(OH)_4$ (am) or $NpO_2\,xH_2O$(am)	0.7	(22)
	$Np^{4+} + 2H_2O(l) - 4H^+ = NpO_2$(cr)	7.7	(22)
	$NpO_2^+ + H_2O(l) - H^+ = NpO_2OH$ (am, aged)	-4.6	(29)
	$NpO_2^+ + H_2O(l) - H^+ = NpO_2OH$ (am, fresh)	-5.2	(29)
	$2NpO_2^+ + H_2O(l) - 2H^+ = Np_2O_5$ (c)	-8.0	(29)
Pu	$Pu^{3+} + 3H_2O - 3H^+ = Pu(OH)_3$ (cr)	-15.8	(14)
	$Pu^{4+} + 4H_2O - 4H^+ = Pu(OH)_4$ (am)	2.5	(22)
	$Pu^{4+} + 2H_2O - 4H^+ = PuO_2$ (cr)	8.0	(22)
	$PuO_2^+ + H_2O(l) - H^+ = PuO_2OH$(am)	-5.0	(14)
	$PuO_2^{2+} + 2H_2O(l) - 2H^+ = PuO_2(OH)_2$(c)	-5.5	(14)
U	$U^{4+} + 2H_2O(l) - 4H^+ = UO_2$(c) (uraninite)	4.9	(22)
	$U^{4+} + 2H_2O(l) - 4H^+ = UO_2$(am)	-1.5	(22)
	$UO_2^{2+} + 3H_2O(l) - 2H^+ = UO_3(c).2H_2O$ (c) (schoepite)	-5.4	(28)
	$2UO_2^{2+} + SiO_2(aq) + 4H_2O(l) - 4H^+ = (UO_2)_2SiO_4 2H_2O$ (soddyite)	-6.0	(27)
	$UO_2^{2+} - H^+ + HCO_3^- = UO_2CO_3$ (rutherfordine)	4.1	(13)
	$2UO_2^{2+} + 2Na^+ + 3H_2O(l) - 6H^+ = Na_2U_2O_7$	-22.6	(30)

* $H^+ + CO_3^{2-} = HCO_3^-$, log K= 10.33

Table 4. Solubility-limiting Solid Phase(SLSP) and Solubility of Actinides Under the Conditions of Present Groundwater

G/W / Actinides		J1 (pH=9.1,	K1 (pH=10.1, Eh=-0.13V)	K2 (pH=10.1, Eh=-0.23V)	K3 (pH=9.9, Eh=-0.16V)	Other works [1] [Ref.] Eh=-0.19V)
Am	Solubility	1.3E-9	2.2E-10	1.9E-10	4.3E-10	6.E-8 [5],
	SLSP	$AmOHCO_3$(c)	$Am(OH)_3$(s)	$Am(OH)_3$(s)	$AmOHCO_3$(c)	3.E-9 [21]
U	Solubility	1.24E-4	7.0E-6	5.6E-6	1.0E-5	4.E-10 [5],
	SLSP	Soddyite	$Na_2U_2O_7$(c)	$Na_2U_2O_7$(c)	$Na_2U_2O_7$(c)	7.4E-8 [21]
Np	Solubility	1.3E-8	3.5E-9	3.1E-9	4.4E-9	2.E-12 [5], 2.E-9 [6], 4.E-8 [7]],
	SLSP	$Np(OH)_4$(am)	$Np(OH)_4$(am)	$Np(OH)_4$(am)	$Np(OH)_4$(am)	2.E-9 [8], 2.5E-10 [21]
Pu	Solubility	2.4E-10	7.1E-11	6.6E-11	8.6E-11	3.E-11 [5],
	SLSP	$Pu(OH)_4$(am)	$Pu(OH)_4$(am)	$Pu(OH)_4$(am)	$Pu(OH)_4$(am)	9.E-11 [21]

1) [5]: pH=8.7, Eh=-0.28V; [6]: pH=6.9, Eh=-0.2V; [7]: pH=8.2, Eh=-0.3V; [8]: pH=7.8, Eh=-0.35V; [21]: pH=9.95, Eh=-0.54V

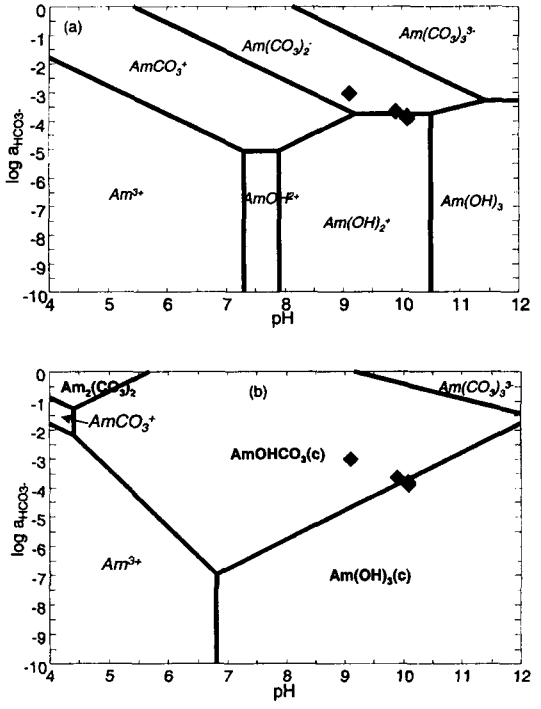

Fig. 1. Speciation of Am(III) as Functions of Carbonate Concentration and pH; (a) Aqueous Species and (b) Solid Stability Fields

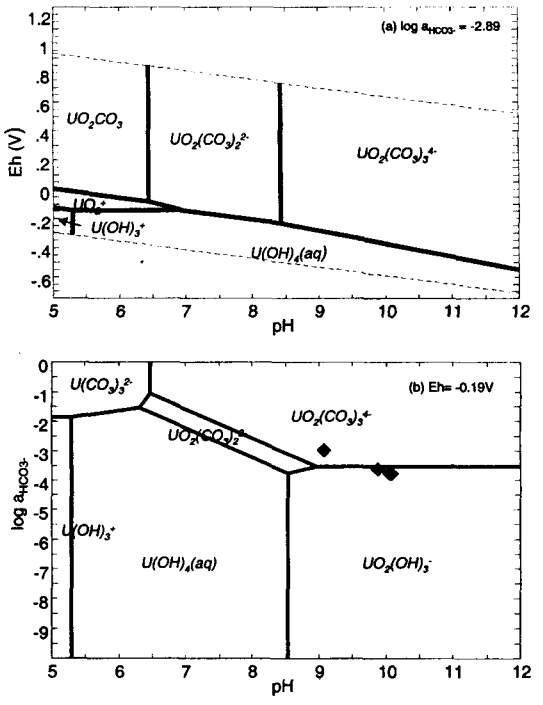

Fig. 2. Aqueous Speciation of U; (a) Eh -pH Diagram (log a_{HCO3-} =-2.89) and (b) HCO_3^--pH Diagram (Eh= -0.19V)

dominant region of $Am(CO_3)_2$ and $Am(OH)_2^+$, respectively. $AmOHCO_3$(s) appears a stable solid phase in J1 and K3 groundwaters, and $Am(OH)_3$(s) in K1 and K2 groundwaters. The different result of the stable solid phase is attributed to the difference in carbonate concentration and pH between groundwaters.

The solubilities of Am under the present groundwater conditions are given in Table 4. The Am solubility of J1 groundwater is 3 or 5 factors higher than those of KAERI site groundwater. Since the Am-carbonate is predominant in the present groundwaters, J1 groundwater with a relatively high carbonate concentration has higher solubility. The Am solubilities of KAERI site groundwater agree within one order of magnitude with the concentration obtained from spent fuel dissolution experiments, which were carried out in a hot cell of a non-oxic atmosphere (21).

3.2. Uranium

Uranium has generally oxidation state ranging from IV to VI, and its speciation varies strongly with pH, Eh and carbonate concentration. An example of Eh-pH diagram for uranium aqueous speciation is given in Figure 2(a) (log a_{HCO3^-} = -2.89, corresponding to J1 groundwater condition). The dashed line represents the stable range of water at 25℃ and 1.013 bar. The species of U(IV) are predominant in reducing condition. Under a very strong reducing condition, the hydroxo-complexes of U(IV), mostly $U(OH)_4$(aq), is predominant in the pH range of environmental groundwater. However, the U(IV)-

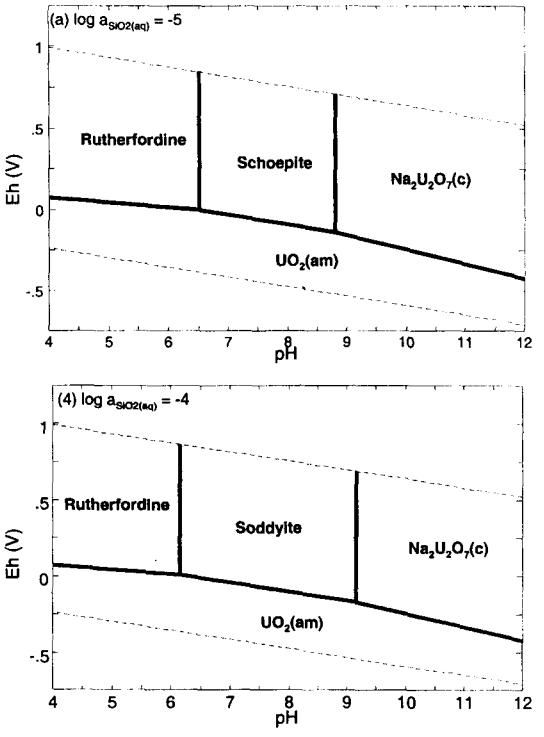

Fig. 3. Stability Diagrams of Uranium Solids for Two Different Silicate Concentrations; (a) log $a_{SiO2(aq)}$ = -5 and (b) log $a_{SiO2(aq)}$ = -4

carbonate is not observed in natural groundwater due to its very low concentration. The U(VI)-carbonate or hydroxo-complexes of U(VI) is predominant in oxidizing condition. In the range of intermediate level of Eh, both oxidation states of U(IV) and U(VI) coexist. Figure 2(b) shows the dependence of dissolved uranium species with pH and carbonate concentration at Eh of -0.19V corresponding to K3 groundwater condition. The dominating aqueous species changes from the hydroxo-complex of U(VI) into U(VI)-carbonate in strong alkaline region, and from the hydroxo-complex of U(IV) into U(VI)-carbonate between weak acidic and weak alkaline region, with increasing carbonate concentration. It appears that $UO_2(CO_3)_3^{4-}$ is the dominant aqueous species in Jungwon groundwater. The KAERI site groundwater lies in near the boundary of region where $UO_2(CO_3)_3^{4-}$ and $UO_2(OH)_3^-$ is predominant, respectively.

The stable solid phase of uranium is strongly dependent on the groundwater conditions. Figure 3 shows the stability diagrams of uranium solids for two the silicate concentrations. The rutherfordine ($UO_2(CO_3)_2(s)$) is a stable solid in oxidizing and low pH region. However, it is not observed in a low carbonate concentration. In high pH $Na_2U_2O_7(c)$ appears a stable solid phase. We can see the different stable solid phase in the range of intermediate pH, where soddyite ($(UO_2)_2SiO_4 \cdot 2H_2O$) or schoepite ($UO_32H_2O$) can be a stable solid, depending on the silicate concentration. The stability diagrams of uranium solids as functions of pH and the silicate concentration are given in Figure 4 at four different reducing conditions, respectively. Based on the thermodynamic data used in the present study, soddyite is more stable if the silicate concentration is greater than 1.95E-5 mol/L (log $a_{SiO2(aq)}$ = -4.71) (Figure 4(a)). The reference value is independent of pH and carbonate concentration. In the groundwater with the silicate concentration less than the reference value, schoepite will be a stable solid phase. However, schoepite appears no longer stable solid phase when the value of Eh is less than about -0.14V (Figures 4(b) to 4(d)). In this case soddyite or $Na_2U_2O_7(c)$ would be a stable solid phase of U(VI). In Jungwon groundwater the stable solid phase of uranium is soddyite, and in KAERI site groundwater it is $Na_2U_2O_7(c)$. On the other hand, uraninite ($UO_2(c)$) or UO_2(fuel) has been assumed to be solubility limiting solid phase of U(IV) in neutral and alkaline region under reducing condition (5,6,8). However, a recent study by Neck and Kim(22) showed that the actinide (IV) in amorphous state would limit its solubility in neutral and alkaline pH region. According to their analysis, the measured

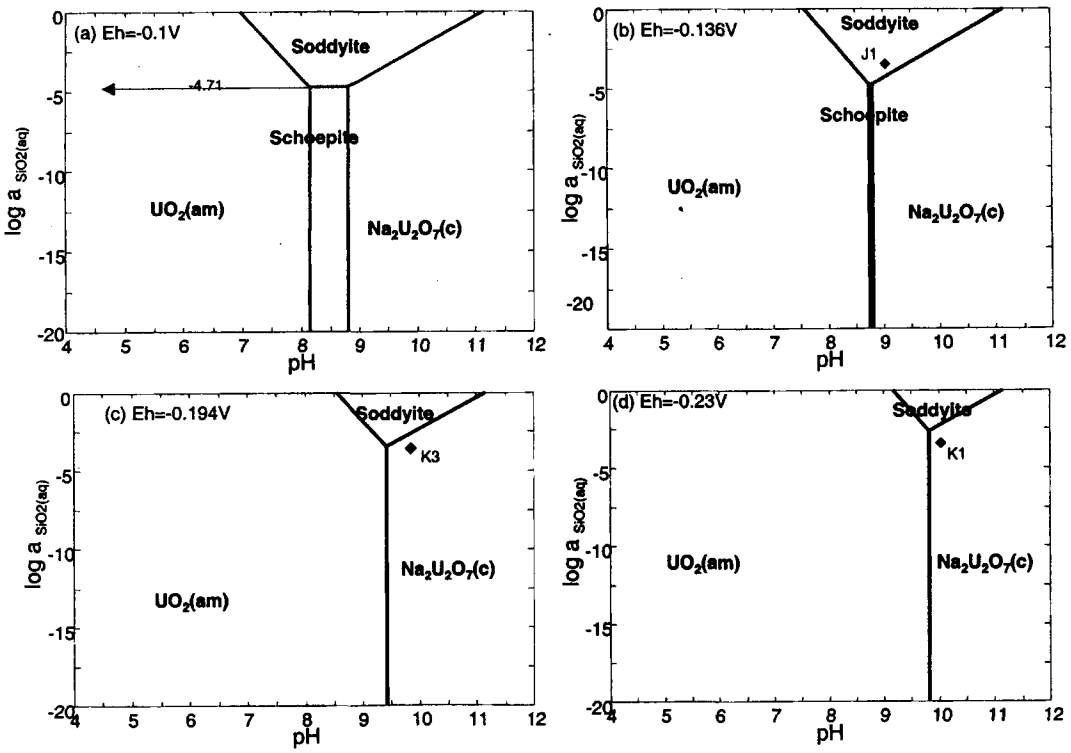

Fig. 4. Stability Diagrams of Uranium Solids as Functions of Silicate Concentration and pH at Different Eh Values; (a) Eh=-0.1V, (b) Eh=-0.136V, (c) Eh=-0.194V, and (d) Eh=-0.23V

solubilities were independent of whether actinides dioxide, AnO_2(cr) or amorphous hydrous oxides ($AnO_2.xH_2O$(am)), was used as the initial solid phase, although the solubility products of the crystalline An(IV) dioxides are about 6-7 orders of magnitude lower than those of the amorphous hydroxides. This was explained by that a bulk crystalline dioxide would be covered with an amorphous surface layer equilibrated with aqueous species in solution. The crystalline An(IV) solid remains the solubility-limiting solid only at very low pH, where An^{4+}(aq) is the predominant aqueous species. Therefore, it is reasonable that the amorphous UO_2(am) would be a solubility-limiting phase of U(IV) in neutral and alkaline region, under reducing condition.

The solubilities of U under the present groundwater conditions are given in Table 4. Almost the same solubility is obtained for KAERI site groundwater conditions, ranging 5.6E-6 to 1.0E-5 mol/L. The uranium solubility of Jungwon groundwater is about one or two orders of magnitude higher than those of KAERI site groundwater, which is the result of the different solubility limiting solid phase between groundwaters. The present solubilities of U are very higher than results obtained by other works (5,21). This discrepancy is attributed to the different groundwater condition of each study, as the solubility of U is particularly sensitive to pH and Eh.

3.3. Neptunium

Within the environmental pH and Eh, it is the IV

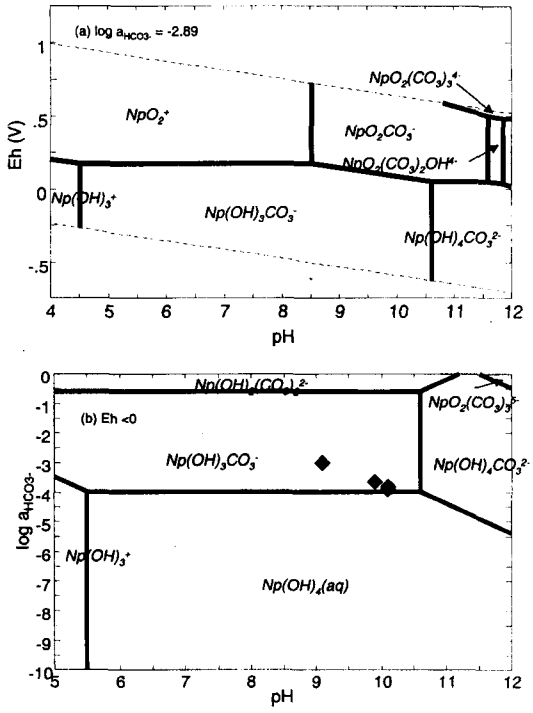

Fig. 5. Aqueous Speciation of Np; (a) Eh -pH Diagram (log a_{HCO3-} =-2.89) and (b) HCO_3^--pH Diagram (Eh<0V)

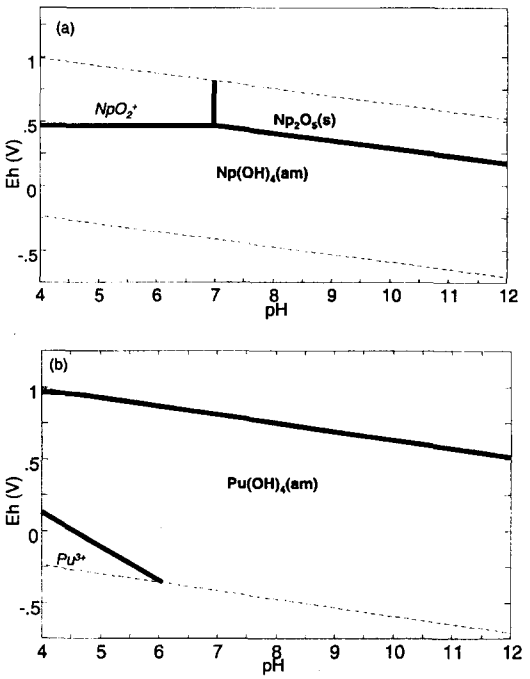

Fig. 6. Solid Stability Diagram of (a) Np and (b) Pu Solids as Functions of pH and Eh

and V oxidation states of neptunium, which are in existence. The neptunium species is greatly influenced by pH and Eh of groundwater as shown in Figure 5(a). Under reducing condition, the complexes of Np(IV) is predominant over pH region of natural groundwater. When the redox potential shifts to oxidizing condition, the dominant aqueous species changes into hydroxo-complexes of Np(V) or Np(V)-carbonate. The carbonate concentration also gives an influence on the dissolved Np species (Figure 5(b)). The diagram has been calculated under reducing condition (Eh<0). In the range of pH between 5.5 and 10.5, the dominating aqueous species changes from $Np(OH)_4(aq)$ to $Np(OH)_3CO_3^-$ with increasing carbonate concentration. In J1 groundwater $Np(OH)_3CO_3^-$ is predominant, whereas in KAERI site groundwater both $Np(OH)_3CO_3^-$ and $Np(OH)_4(aq)$ appear significant species. In Figure 6(a) we can see that $Np(OH)_4(am)$ is a stable solid phase in a wide region of pH and Eh. When Eh is a very high, $Np_2O_5(s)$ appears a stable solid in neutral and alkaline region.

The solubilities of Np under the present groundwater conditions are given in Table 4. The solubilities are almost constant, ranging 3.1E-9 to 1.3E-8 mol/L. Generally, the solubility of Np is independent of pH and Eh, under natural deep granitic groundwater conditions, because $Np(OH)_3CO_3^-$ is mostly the predominant species. In such a case the carbonate concentration in solution is the dominant factor determining the solubility. The relatively higher Np solubility of J1 groundwater is the result of its higher carbonate

concentration. The present solubilities of Np agree well within one order of magnitude with results by SKB(6), SKI(7) and TVO(8) as well as experimental data by Grambow et al. (21). However, those are three to four orders of magnitude higher than the result by PNC(5), which seems to be caused by either the different thermodynamic data used or more probably, the different solubility limiting solid phase between both studies.

3.4. Plutonium

The plutonium exists mostly as the III or IV states in deep groundwater condition. Figure 7(a) shows the dependence of the Pu aqueous speciation with pH and Eh. The species of Pu(III) are predominant in acidic regon, and the species of Pu(IV) in neutral and alkaline region. The area where the species of Pu(III) are predominant widens with decreasing pH and Eh. The species of Pu(V) are the dominating species under a strong oxidizing condition. As in the case of other actinides studied, the speciation of Pu is also very sensitive to carbonate concentration (Figure 7(b)). The diagram has been calculated under reducing condition (Eh<0). In alkaline pH region the predominant aqueous species changes from $Pu(OH)_4(aq)$ into $Pu(OH)_3CO_3^-$ with increasing carbonate concentration, whereas in acidic and neutral pH region the hydroxo-complexes of Pu(III) are predominant over a wide range of carbonate concentration. J1 groundwater is in the region where $Pu(OH)_3CO_3^-$ is predominant, and K1 and K2 groundwaters are in the region where $Pu(OH)_4(aq)$ is predominant. In K3 groundwater both $Pu(OH)_3CO_3^-$ and $Pu(OH)_4(aq)$ appear all much the same in significance.

In natural groundwater condition it appears that $Pu(OH)_4(am)$ is the most stable solid phase of Pu

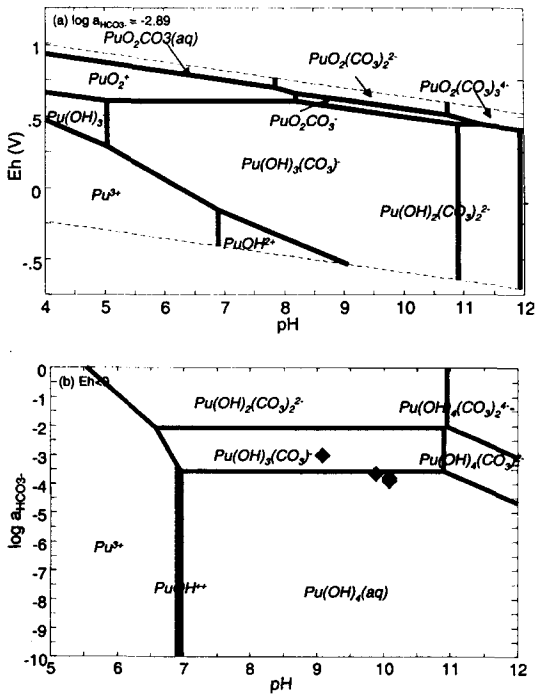

Fig 7. Aqueous Speciation of Pu; (a) Eh -pH Diagram (log a_{HCO3^-} =-2.89) and (b) HCO_3^--pH diagram (Eh<0V)

(Figure 6(b)). The calculated solubilities of $Pu(OH)_4(am)$ under the present groundwater conditions are given in Table 4. The Np solubility of J1 groundwater is about three factors higher than those of KAERI site groundwater, due to the higher carbonate concentration of J1 groundwater. The present solubilities of Pu agree well with the results of other studies obtained with similar pH condition (5, 21).

4. Conclusions

The speciation and solubility of Am, U, Np and Pu under the conditions of the domestic deep groundwaters have been analyzed by means of the geochemical code MUGREM and the

thermodynamic data selected through literature review. The groundwaters were sampled from Jungwon (Chungbuk) and KAERI site (Yuseong, Daejeon), respectively.

Under the conditions of groundwaters studied, the stable solid phase is $AmOHCO_3$(s) or $Am(OH)_3$(s), soddyite or $Na_2U_2O_7$(c), $Np(OH)_4$(am), and $Pu(OH)_4$(am) for Am, U, Np, and Pu, respectively. The dominating aqueous species are as follows: the complexes of Am(III), $Am(OH)_2^+$ and $Am(CO_3)_2^-$, the complexes of U(VI), $UO_2(OH)_3^-$ and $UO_2(CO_3)_3^{4-}$, the complexes of Np(IV), $Np(OH)_4$(aq) and $Np(OH)_3CO_3^-$, and the complexes of Pu(IV), $Pu(OH)_4$(aq) and $Pu(OH)_3CO_3^-$. The solubilities of the present study exist between 1.9E-10 and 1.3E-9 mol/L for Am, between 5.6E-6 and 1.2E-4 mol/L for U, between 3.1E-9 and 1.3E-8 mol/L for Np, and between 6.6E-10 and 2.4E-10 mol/L for Pu. The solubilities agree well with the results of other studies obtained under similar conditions.

Conclusively, the speciation and solubility of actinides are very sensitive to carbonate concentration, pH and Eh. Therefore, caution should be taken in the measurement of groundwater compositions in order to accurately consider in-situ condition. Also, viewed in the radiological importance of actinides in safety assessment, their thermodynamic data should be continuously upgraded.

Acknowledgements

This study has been supported by the Nuclear Research Program of MOST, Korea.

References

1. OECD/NEA, *Geological Disposal of Radioactive Waste: An Overview of the Current Status of Understanding and Development*, OECD/NEA, p.111, (1984).
2. Dormuth, K.W., "Assessment of the Canadian Nuclear Fuel Disposal Concept," *Proceeding of Symposium on Safety Assessment of Radioactive Waste Repositories*, OECD/NEA, 211 (1993).
3. Golder Associates, *Performance Evaluations Related to Area Characterization of Crystalline Rock*, Golder Associates, Office Crystalline Repository Division, OH, BMI/OCRD-27, (1988).
4. Nagra, *Project Gewahr 1985*, Nagra, Baden, Project Report, NGB 85-09, (1985).
5. PNC, *Research and Development on Geological Disposal of High-Level Radioactive Waste: Final Progress Report*, PNC, Tokyo, Tech. Report, TN1410 93-018, (1992).
6. SKB, SKB-91; *Final Disposal of Spent Nuclear Fuel- Importance of the Bedrock for Safety*, SKB, Stockholm, Tech. Report, TR 92-20, (1992).
7. SKI, *SKI Project 90 Summary, SKI*, Stockholm, Tech., Report 91-23, (1991).
8. TVO, *Final Disposal of Spent Nuclear Fuel in Finnish Bedrock*, YJT, Helsinki, Tech. Report YJT-92-31E, (1992).
9. Keum, D.K. and P.S Hahn, "Application and Development of a Multi-geochemical Reaction Equilibrium Model (MUGREM)," *Environ. Eng. Res.*, 4, 113(1999).
10. Bond, K.A., T.G. Heath, and C.J. Tweed, HATCHES: *A Reference Thermodynamic Database for Chemical Equilibrium Studies*. Nirex, Switzerland, Report NSS/R379, December (1997).
11. Fuger, J., I.L. Khodakovsky, E.I. Sergeyeva, V.A. Medvedev and J.D. Narvratil, *The Chemical Thermodynamics of Actinide Elements and Compounds, Part 12; The Actinide Aqueous Inorganic Complexes*,

IAEA, Vienna, Austria, (1992).

12. Frlmy, A.R., D. Girvin, and E.A. Jenne, *MINTEQ: A Computer Program for Calculating Aqueous Geochemical Equilibria,* U.S. Environmental Protection Agency, by Battelle, Pacific Northwest Laboratories, Richland, Washington, EPA-600/3-84-032, (1984).
13. Grenthe, I., J. Fuger, R.J.M. Konings, R.J. Lemire, A.B. Muller, C.N. Gregu, and H. Wanner, *Chemical Thermodynamics Series 1: Chemical Thermodynamics of uranium*: NEA-TDB, OECD, p.715, North Holland Elsevier Science Publishers, (1992).
14. Lemire, R.J., J. Fuger, H. Nitsche, P. Potter, M.H. Rand, J. Rydberg, K. Spahin, J.C. Sullivan, W.J. Ullman, P. Vitorge, and H. Wanner, *Chemical Thermodynamics Series 4: Chemical Thermodynamics of Neptunium and Plutonium*: NEA-TDB, OECD, p.845, North-Holland Elsevier Science Publishers, (2001).
15. Pearson, F.J. and H.N. Waber, NAGRA/PSI Thermodynamic Data Base: *Preparation of a Version for PHREEQC*, NAGRA, Switzerland, TM-44-99-01, (1999).
16. Silva, R.J., G. Bidoglio, M.H. Rand, P.B. Robouch, H. Wanner, and I. Puigdomenech, *Chemical Thermodynamics Series 2: Chemical Thermodynamics of Americium: NEA-TDB, OECD*, p.374, North-Holland Elsevier Science Publishers, (1995).
17. Wolery, T.J., *Calculation of Chemical Equilibrium between Aqueous Solutions and Minerals: The EQ3/6 Software Package*, Lowrence Livermore National Lab., Livermore, CA, UCRL-52658, (1992).
18. Keum, D.K., M.H. Baik and P.S. Hahn, *Thermodynamic data of Am, Th, U, Np and Pu and their application for HLW disposal, KAERI, Technical report, KAERI/TR-2046/02*, (2002).
19. Neck, V. and J.I. Kim, "Thermodynamics of Tetravalent Actinides: A Critical Assessment of Uncertainties," *Proceeding of Actinides Conferences 2001, Hajiyama*, Japan, (2001).
20. Takeda, S., S. Shima and H. Kimura, *The aqueous solubility and speciation analysis for uranium, neptunium and selenium by the EQ3/6*, JAERI research 95-069, (1995).
21. Grambow, B., A. Loida, A. Martinez-Esparza, P. Diaz-Arocas, J. de Pablo, J.L. Paul, G. Marx, J.P. Glatz, K. Lemmens, K. Ollila, and H. Christensen, *Long-term Safety of Radioactive Waste Disposal: Source Term for Performance Assessment of Spent Fuel as a Waste Form*, Final Report, Forschungszentrum Karlsruhe, Germany, FZKA 6420, (2000).
22. Neck, V. and J.I Kim, "Solubility and Hydrolysis of Tetravalent Actinides," *Radiochimica Acta*, 89, 1(2001).
23. Neck, V. and J.I. Kim, "An Electrostatic Approach for the Prediction of Actinide Complexation Constants with Inorganic Ligands-Application to Carbonate Complexes," *Radiochimica Acta*, 88, 815(2000).
24. Neck, V. and V. Metz, *Kenntnisstand zur Aquatischen Chemie und Thermodynamik von Hexavalenten Actiniden*, Forschungszentrum, Karlsruhe, Germany, FZK/INE 010/00 (internal report, unpublished), (2001).
25. Neck, V., W. Runde, J.I. Kim and B. Kanellakopulos, "Solid-Liquid Equilibrium Reactions of Neptunium(V) in Carbonate Solution at Different Ionic Strength," *Radiochimica Acta*, 65, 29(1994).
26. Neck, V., Th. Fanghanel, and J.I. Kim, *Aquatische Chemie und Thermodynamische Modellierung von Trivalenten Actiniden*, Forschungszentrum Karlsruhe, Germany,

FZKA 6110, (1998).

27. Moll, H., G. Geipel, W. Metz, G. Bernhard, and H. Nitsche, "Solubility and Speciation of $(UO_2)_2SiO_42H_2O$ in Aqueous Systems," *Radiochimica Acta*, 74, 3(1996).
28. Dpeiaz, A.P. and B. Grambows, "Solid-Liquid Phase Equilibria of U(VI) in NaCl Brines," *Geochim. Cosmochim Acta*, 62, 236(1998).
29. Fanghanel, Th., V. Neck and J.I. Kim, "Thermodynamics of Neptunium(V) in Concentrated Salt Solutions: II.Ion Interaction (Pitzer) Parameters for Np(V) Hydrolysis Species and Carbonate Complexes," *Radiochimica Acta*, .69, 169(1995).
30. Sandino, A., and B. Grambow, "Solubility Equilibria in U(VI)-Ca-K-Cl-H_2O System: Transformation of Schoepite into Becquerelite and Compreignacite," *Radiochmica Acta*, 66/67, 37(1994).